

Modelling Circumbinary Gas Flows in Close T Tauri Binaries^{*}

M. de Val-Borro,^{1†} G. F. Gahm,² H. C. Stempels,³ and A. Pepliński²

¹*Max Planck Institute for Solar System Research, DE-37191 Katlenburg-Lindau, Germany*

²*Stockholm University, AlbaNova University Center, SE-10691, Stockholm, Sweden*

³*Department of Physics and Astronomy, Uppsala University, Box 515, SE-75120 Uppsala, Sweden*

Received May 10, 2010;

ABSTRACT

Young close binaries open central gaps in the surrounding circumbinary accretion disc, but the stellar components may still gain mass from gas crossing through the gap. It is not well understood how this process operates and how the stellar components are affected by such inflows. Our main goal is to investigate how gas accretion takes place and evolves in close T Tauri binary systems. In particular, we model the accretion flows around two close T Tauri binaries, V4046 Sgr and DQ Tau, both showing periodic changes in emission lines, although their orbital characteristics are very different. In order to derive the density and velocity maps of the circumbinary material, we employ two-dimensional hydrodynamic simulations with a locally isothermal equation of state. The flow patterns become quasi-stable after a few orbits in the frame co-rotating with the system. Gas flows across the circumbinary gap through the co-rotating Lagrangian points, and local circumstellar discs develop around both components. Spiral density patterns develop in the circumbinary disc that transport angular momentum efficiently. Mass is preferentially channelled towards the primary and its circumstellar disc is more massive than the disc around the secondary. We also compare the derived density distribution to observed line profile variability. The line profile variability tracing the gas flows in the central cavity shows clear similarities with the corresponding observed line profile variability in V4046 Sgr, but only when the local circumstellar disc emission was excluded. Closer to the stars normal magnetospheric accretion may dominate while further out the dynamic accretion process outlined here dominates. Periodic changes in the accretion rates onto the stars can explain the outbursts of line emission observed in eccentric systems such as DQ Tau.

Key words: Accretion, accretion discs – binaries: close – hydrodynamics – methods: numerical – stars: individual: V4046 Sgr, DQ Tau – stars: pre-main sequence.

1 INTRODUCTION

Classical T Tauri stars (CTTS) are young pre-main-sequence objects with pronounced emission line features and an infrared excess indicative of dust in the circumstellar discs. A number of CTTS are confirmed close binaries, with orbital periods from days to weeks, and several of these show emission lines that vary in intensity and line shape with phase. In such systems, the stars orbit in a gap opened by tidal interactions inside a circumbinary disc. Eccentric systems, like DQ Tau (Basri et al. 1997) and UZ Tau E (Martín et al. 2005), show enhanced emission line activity

close to periastron passages. This indicates that the accretion in such systems is non-axisymmetric, and perturbed by the orbital interaction with the inner disc. However, in at least one system with equal-mass components and nearly circular orbits, namely V4046 Sgr, emitting gas fills the gap between the stars and the surrounding disc. Observations of V4046 Sgr by Stempels & Gahm (2004) provided evidence that the flows are manifestations of non-axisymmetric mass accretion in this system. These observations show that gas flows across the gap also in young, close binary systems with circular orbits.

Circumbinary discs are common in a wide range of astrophysical objects such as young binary stellar systems and massive binary black hole systems at the centre of galaxies (see e.g. Hayasaki et al. 2007). Binary stars are believed to form by fragmentation of dense cores and accrete mass from

^{*} Based on observations collected at the European Southern Observatory.

[†] E-mail: deval@mps.mpg.de

the envelope via a circumbinary disc. It is of interest to understand how the components in binaries evolve due to preferential mass accretion, and how the orbital elements may change with time. Protobinary systems allow us to study disc evolution under well defined conditions, since the sizes of the central gaps in the circumbinary disc are determined by tidal truncation and the stellar components are supposed coeval. The common evolution of the circumstellar discs is governed by accretion from the circumbinary disc that can extend up to hundreds of AU.

Numerical simulations of binary systems with a circumbinary disc based on Smoothed Particle Hydrodynamics (SPH) (Artymowicz & Lubow 1994; Bate & Bonnell 1997) and grid-based methods (Günther & Kley 2002; Günther et al. 2004) show that an inner cavity forms inside of the 2:1 resonance. Bate & Bonnell (1997) found that, in binaries with a mass ratio different from unity, the less massive protostar accretes more material and is therefore more luminous. However, that claim has been later refuted using high-resolution two-dimensional grid-based simulations (Ochi et al. 2005; Sotnikova & Grinin 2007; Hanawa et al. 2010). Recent SPH simulations of multiple star formation in molecular clouds have shown that unequal mass binaries are rare (Delgado-Donate et al. 2004; Clarke 2008), although observational data indicates that mass ratios different from unity are common (Reid & Gizis 1997). For reviews of observational properties and numerical simulations of young multiple systems see Mathieu et al. (2000); Duchêne et al. (2007); Goodwin et al. (2007).

Artymowicz & Lubow (1996) found that binaries with eccentric orbits can generate non-axisymmetric gas flows from the disc edge in agreement with the periodic line changes observed in such systems. Preliminary simulations of systems with circular orbits (Artymowicz 2005 – see Gahm 2006, page 151), have shown that mass accretion occurs, but the gas density inside the gap is much lower than for systems with eccentric orbits. Such simulations, and with similar conclusions, were later done by Sotnikova & Grinin (2007). Systems with companions on inclined circular orbits have also been modelled (Papaloizou & Terquem 1995).

In the present paper we investigate accretion in close T Tauri binaries and follow the early stages of their evolution. We carry out numerical simulations of protoplanetary discs surrounding close T Tauri binaries using an Adaptive Mesh Refinement (AMR) scheme, providing high spatial resolution inside the inner cavity opened by the binary orbit. We follow the formation of a circumstellar gap in the disc and map the accretion flows onto the stellar components where local circumstellar accretion discs form, and estimate line profile emission from the accretion flows. We select the orbital parameters of the systems to match two well observed spectroscopic binary systems V4046 Sgr (circular) and DQ Tau (eccentric) in order to compare the accretion process in these two different cases, and we explore how our results compare with earlier simulations of similar systems. Observations indicate that accretion from such circumbinary discs occurs over the gap but that the gas flows are non-axisymmetric. The stellar components in these systems gain most of their mass by accretion through circumstellar discs. Our calculations also provide information on whether mass accretion is directed preferentially to the primary or the secondary in the different systems. In order to shed some

light on this question we have also modelled a system on a circular orbit, but with a mass ratio different from unity. Finally, both V4046 Sgr and DQ Tau show remarkable periodic changes in the Balmer line profiles. We explore in a qualitative way to what extent these variations could match predictions from our model. This study is also relevant to understand accretion onto a planet that is massive enough to tidally open a gap in a circumstellar disc. Giant planets can accrete material outside the planet’s orbit through the annular cavity at a rate comparable with the accretion rate onto the inner disc (Kley et al. 2001).

This paper is organized as follows. Our physical model and numerical code are described in Section 2. The main results from our simulations of circular and eccentric binary systems are presented in Section 3, and comparisons to observed emission line variations in V4046 Sgr and DQ Tau are made in Section 4, where we also discuss differences between accretion in systems with different mass ratios. Finally, the conclusions are given in Section 5.

2 NUMERICAL SETUP

We consider the evolution of a non-self-gravitating circumbinary disc around close T Tauri binary systems with circular and eccentric orbits. First, we model a circular system with parameters similar to the T Tauri system V4046 Sgr, for which we have acquired complementary observations. The parameters stellar mass, semi-major axis, period, inclination and eccentricity are given in Table 1. In the second set of simulations we study close binary systems with moderate orbital eccentricity and mass ratio close to unity such as DQ Tau (see Table 2). There is observational evidence that both system are surrounded by extensive circumbinary discs (see Stempels & Gahm 2004; Mathieu et al. 1997; Kastner et al. 2008, for details).

2.1 Basic equations

The system is described by the two-dimensional Navier-Stokes equations using vertically-integrated variables

$$\frac{\partial \Sigma}{\partial t} + \nabla \cdot (\Sigma \mathbf{v}) = 0 \quad (1)$$

$$\frac{\partial \mathbf{v}}{\partial t} + (\mathbf{v} \cdot \nabla) \mathbf{v} = -\frac{1}{\Sigma} \nabla P - \nabla \Phi \quad (2)$$

Σ denotes the surface density, P is the pressure, \mathbf{v} is the velocity of the fluid and Φ is the gravitational potential. The surface density can be expressed as

$$\Sigma(r, \phi) = \int_{-\infty}^{\infty} \rho(r, \phi, z) dz, \quad (3)$$

where ρ is the three-dimensional density. The gravitational potential is given by the formula

$$\phi(r, t) = \sum_{i=1}^2 \phi_i(r, t). \quad (4)$$

Each stellar component has a potential of the form

$$\phi_i = \frac{-GM_i}{\sqrt{(r - r_i)^2 + \epsilon^2}}, \quad (5)$$

Table 1. Orbital parameters of the circular binary system V4046 Sgr (Stempels & Gahm 2004; Quast et al. 2000). Masses are in units of the solar mass and distances are in solar radii.

Parameter	Primary	Secondary
M	$0.912 M_{\odot}$	$0.873 M_{\odot}$
a_1, a_2	$4.52 R_{\odot}$	$4.72 R_{\odot}$
P	2.4213459 d	
i	35°	
e	≤ 0.01	

where ϵ is the gravitational softening, r is the distance from the centre of mass and r_i denotes the position of the star. The softening length is typically $0.1a$ in our simulations. This value is smaller than the Hill radius where the gravity from the star dominates and the gas forms a circumstellar disc. Therefore, the choice of softening length does not affect strongly the results of our simulations.

We adopt a simple equation of state for the gas in our models with a temperature profile depending on the distance to the centre of mass and to each stellar component. A locally isothermal solver for the circumbinary disc with constant aspect ratio $H/r = 0.05$ is implemented, where H is the disc scale height and r is the distance from the barycentre (see e.g., Lin & Papaloizou 1985). The sound speed in the circumbinary disk is given approximately by the formula

$$c_s = H\Omega_d, \quad (6)$$

where H is the scale-height and Ω_d is the Keplerian angular velocity in the circumbinary disc. Each stellar component has a temperature distribution according to the prescription in Pepliński et al. (2008). Accretion processes in circumbinary discs can be an efficient mechanism to convert gravitational potential energy into radiation for high mass accretion rates. In our case, the disc is assumed to radiate efficiently the thermal energy generated from tidal dissipation, viscous heating and stellar radiation. In the absence of an efficient cooling mechanism the gas would heat up and the disc would become geometrically thick. We do not include irradiation effects from the stars in our equation of state.

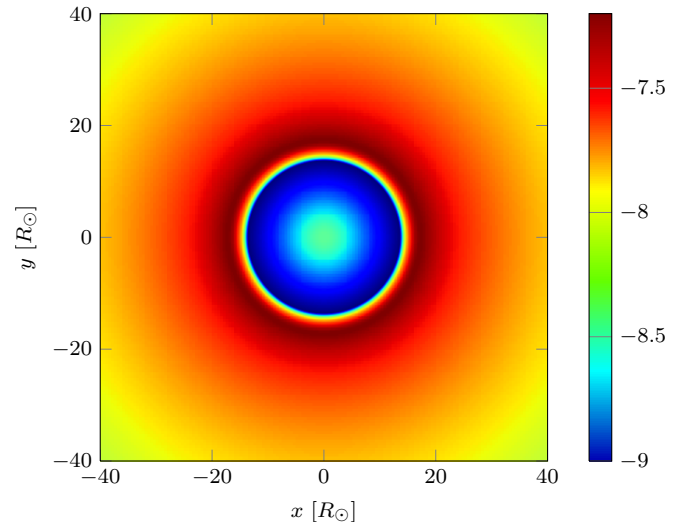
Self-gravity of the disc was not considered in our simulations since the total mass of the disc material in the computational domain is much smaller than the mass of the binary system (see e.g. Günther et al. 2004). Initially, we kept the system in a fixed Keplerian orbit and assumed a coplanar circumbinary disc for simplicity. In some computations, we did not account for the accretion of material onto the stars and therefore a high density peak forms around the stars. Such high-density peaks are clearly an artefact of our simulations and are not real. We therefore exclude these regions when doing a comparison with observations (see Section 4).

2.2 Initial and boundary conditions

The binary orbits and mass ratios assumed in the presented simulations are chosen to closely match the configurations of V4046 Sgr and DQ Tau. At time zero we start with a surface density proportional to $r^{-0.5}$ following Günther & Kley (2002). However, the density distribution at large distances in the circumbinary disc has no appreciable effect on

Table 2. Orbital parameters of the elliptic binary system DQ Tau (Mathieu et al. 1997)

Parameter	Primary	Secondary
M	$0.55 M_{\odot}$	$0.55 M_{\odot}$
a_1, a_2	$6.6 R_{\odot}$	$6.6 R_{\odot}$
P	15.8043 d	
i	23°	
e	0.556	

**Figure 1.** Initial surface density distribution with coordinates expressed in solar radii for the DQ Tau case (see Table 2). The surface density in computational units is given in logarithmic scale. The outer circumbinary disc is represented by the equilibrium distribution of an accretion disc around a single star, where the surface density is proportional to $r^{-0.5}$ (Günther & Kley 2002).

the accretion flows through the gap. We created a central axisymmetric cavity around the centre of mass of the stellar system inside the 2:1 resonance initially, where we have set the density to $\Sigma \approx 10^{-2}\Sigma_0$ in our computational units. The circumbinary gas rotates in the same direction as the stars and initially has Keplerian velocities around the centre of mass of the system. In Fig. 1, we show an example of an initial axisymmetric surface density profile with a power-law radial dependence at large distances. The gravitational potential of the stars is introduced smoothly over half an orbit to avoid the formation of strong shocks.

We used open outflowing boundaries with wave damping zones outside $r = 2a$ to avoid wave reflection and mass loss. Mass inflow into our computational domain was not considered. The damping regions were implemented in the outer regions of the circumbinary disc where the following equation was solved after each time step:

$$\frac{dx}{dt} = -\frac{x - x_0}{\tau} R(r), \quad (7)$$

where x represents either the surface density, or the velocity components, τ is the orbital period of the gas at $r = 2a$ and $R(r)$ is a ramp-up function which becomes unity at $r = 3a$ (de Val-Borro et al. 2006). With this boundary prescription we can avoid mass loss through the open boundaries.

Simulations were run using different damping functions to confirm that the gap structure and accretion streams do not depend strongly on our choice of boundary conditions.

Material from the circumbinary disc is accreted through the gap and forms circumstellar discs. Accretion onto the stars is estimated by removing material from a region inside the Hill radius for each stellar component every time-step (see e.g. Pepliński et al. 2008; de Val-Borro et al. 2009), although the dynamical mass of the stars is kept constant. Since the obtained accretion rates and time scales are small this is a reasonable assumption. The mass is removed from the circumstellar disk after each time step using the expression

$$\Delta\Sigma = \max(0, \Sigma - \Sigma_{\text{av}}), \quad (8)$$

where Σ_{av} denotes the average density in the star's neighbourhood $r_{\text{acc}} < |\mathbf{r} - \mathbf{r}_s| < 2r_{\text{acc}}$, where r_{acc} is a fraction of the softening length. The momentum of the accreted material is removed from the system.

2.3 Numerical code

We performed two-dimensional hydrodynamic simulations of the material in the orbital plane on a Cartesian grid. The simulations were run on a dynamically refined grid for ~ 10 orbital periods when the system has reached a quasi-static configuration.

The Cartesian version of the FLASH code was run in the inertial frame centered on the centre of mass of the binary system. FLASH is a parallel block-structured code based on the Piecewise Parabolic Method (PPM) (Fryxell et al. 2000)¹. The code has been extensively tested in various compressible flow astrophysical problems (see e.g. de Val-Borro et al. 2006, and references therein). FLASH uses the PARAMESH library to refine the grid dynamically based on the behaviour of the solution.

For this work, we explicitly ensure the conservative transport of angular momentum to a high degree of accuracy introducing the Coriolis force as source terms (Kley 1998). This is particularly important when large density gradients are present in the computational domain. In our problem, we need to resolve a large density contrast between the inner cavity and the circumbinary disc. Our implementation includes an adapted equation of state module and a simple N-body solver to evolve the binary orbit. Physical viscosity is not included in our simulations. In addition, FLASH is able to resolve the spiral arms in our simulations and an artificial viscosity is not needed to smooth out the shocks.

The unit of distance is $a = 1$ in the simulations, and the unit of time is the orbital period of the system which is given by

$$P = 2\pi\sqrt{\frac{a^3}{G(M_1 + M_2)}} = 2\pi, \quad (9)$$

where $G(M_1 + M_2) = 1$ for computational convenience. In our units the angular frequency of the binary is $\Omega = 1$.

The number of cells in our simulations is $n_x \times n_y = (256, 256)$ and $n_x \times n_y = (512, 512)$ for the higher-resolution

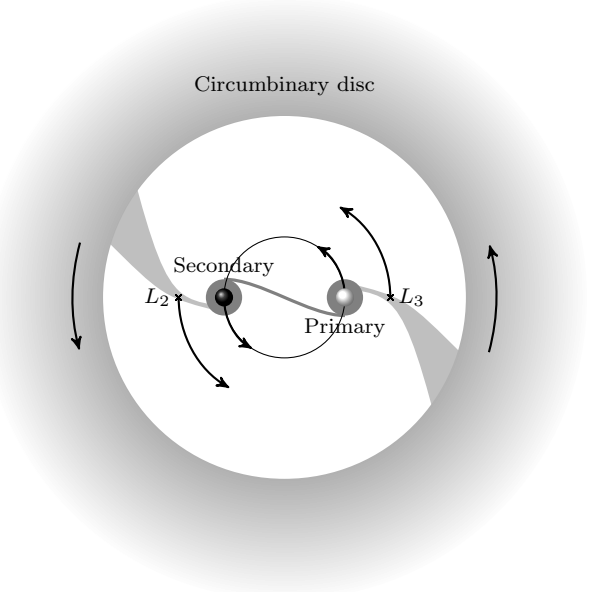


Figure 2. Diagram of a gravitationally bound binary system on a circular orbit surrounded by a circumbinary disc in Keplerian rotation. The gravitational interaction creates a central cavity at the tidal truncation radius. Local circumstellar discs form around each star from material accreted from the circumbinary disc through the Lagrangian points L_2 and L_3 .

simulations, with four additional levels of refinement. Therefore, we achieve high-resolution inside the circumbinary gap and in the vicinity of the stars. The computational domain extends between $-3a \leq x \leq 3a$ and $-3a \leq y \leq 3a$, with uniform spacing in our base grid in both directions.

3 RESULTS

In this section we discuss the results of our simulations of circular and eccentric binary systems surrounded by a circumbinary disc. A central cavity forms on the dynamical scale by the gravitational effect of the binary with the inner edge close to the 2:1 corotation resonance. The disc relaxes viscously on short time scales and the flow becomes quasi-stationary in the corotating frame for circular binaries. This case is also appropriate to test the stability of our numerical method. The accretion flows form global patterns as shown in Fig. 2 for a binary on a circular orbit with a surrounding circumbinary disc after the envelope has been dissipated. Gas streams from the surrounding disc across the central cavity through the co-linear Lagrangian points L_2 and L_3 , and small local discs develop around each star.

3.1 Circular Binaries

After about two orbits, we obtain a quasi-stationary and symmetric configuration in the corotating frame of the system. Figure 3 shows the surface density in logarithmic scale for the V4046 Sgr system after five orbits. At this time, the surface density within the inner hole is reduced about six orders of magnitude relative to the density in the outer disc.

¹ FLASH is available at <http://www.flash.uchicago.edu/>

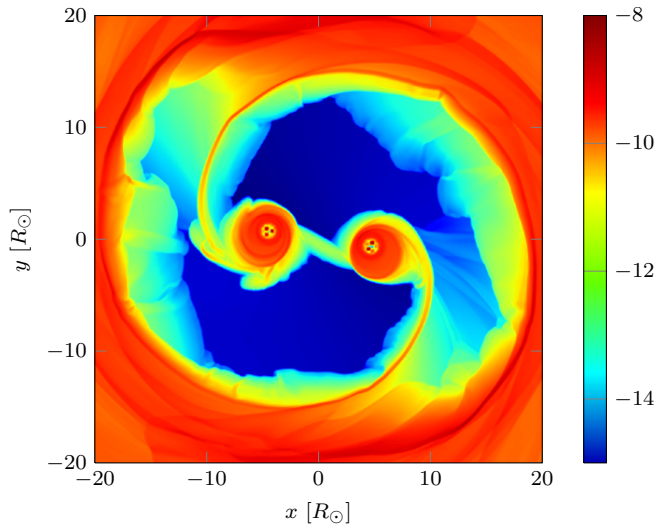


Figure 3. Surface density map in logarithmic scale for a simulation of the system V4046 Sgr after 5 orbits including accretion onto the stars. The initial surface density of the circumbinary disc is unity. The secondary is located at $(x, y) = (-4.72, 0) R_\odot$, and the primary at $(x, y) = (4.52, 0) R_\odot$. The system rotates in counterclockwise direction.

The corresponding velocity pattern is shown in Fig. 4. Figure 5 shows the velocity vectors in the inertial frame, and the corresponding flow lines in the corotating frame are displayed in Fig. 6. Although the numerical viscosity in our code is small (de Val-Borro et al. 2007), diffusion into the inner hole can result from numerical viscosity or shock formation. Still, the tidal gap remains open for the duration of our simulations although significant accretion continues onto the stars.

Two-armed spiral structures form in the circumstellar discs after about one orbit, and a high-density arm joins both discs. The circumstellar discs are strongly perturbed by the accretion flows through the inner cavity, although the spiral arms remain in a stable configuration for the duration of our simulations. The gravitational softening affects the density distribution around the star but it does not modify the accretion flows through the gap.

We have used a grid structure with four additional levels of refinement shown in Fig. 7. Almost the whole inner gap and stellar components are refined and therefore have higher resolution. The outer regions of the disc have coarser resolution which allows us to speed up the calculation. From lower-resolution test runs involving more than 10 orbits we conclude that the pattern of gas flows and the position of the edge of the circumbinary disc do not change significantly after about five orbits.

Figure 8 shows the averaged surface density around the stellar components as a function of radial distance. In this simulation, mass is not accreted onto the stars, and the density peaks in both discs reflect this accumulation of matter. Since mass is not removed from the disc, the profile does not correspond to a standard accretion disc. In addition, the density distribution in the inner disc is influenced by the gravity softening. Therefore, the stellar cores are excluded from the calculation of emission line profiles. The circumbinary disc around the primary is slightly more mas-

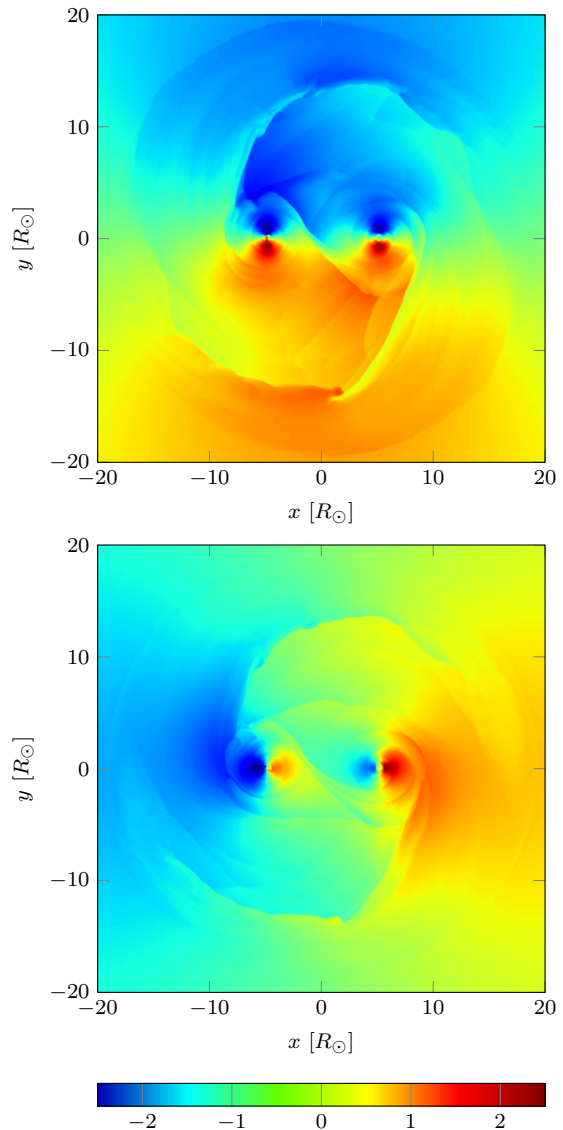


Figure 4. Velocity maps for V4046 Sgr after five orbits. The upper panel shows the v_x component and the lower panel shows the v_y component. The color scale is in units of $a\Omega$.

sive than the disc around the secondary. If mass is accreted in the circumstellar discs, averaged accretion rates onto the stellar cores are $\sim 2.8 \times 10^{-8} M_\odot \text{ yr}^{-1}$. These values agree in order of magnitude with other eccentric and circular binary simulations (Günther & Kley 2002; Günther et al. 2004). Fig. 9 shows the accreted mass onto the primary against time for the V4046 Sgr model.

We then repeat our simulations of a circular binary but with components of different mass. We set the mass ratio to 1:5 with the same primary mass and mean distance between the components as in the V4046 Sgr system. As shown in Fig. 10 circular systems with low mass companions also develop central gaps, non-axisymmetric mass accretion and local circumstellar discs. The averaged mass accretion rate onto the primary is $3.1 \times 10^{-8} M_\odot \text{ yr}^{-1}$, while the averaged mass accretion rate onto the secondary is $2.2 \times 10^{-8} M_\odot \text{ yr}^{-1}$, and the corresponding stellar disc is less massive.

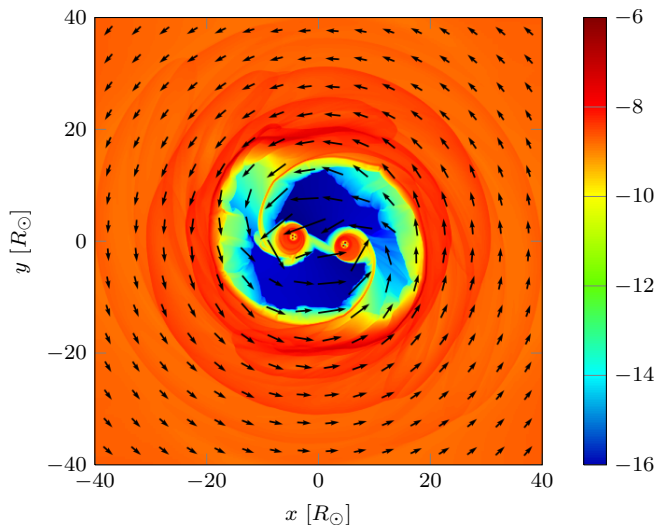


Figure 5. Surface density and velocity distribution denoted by arrows for the same snapshot as shown in Fig. 3.

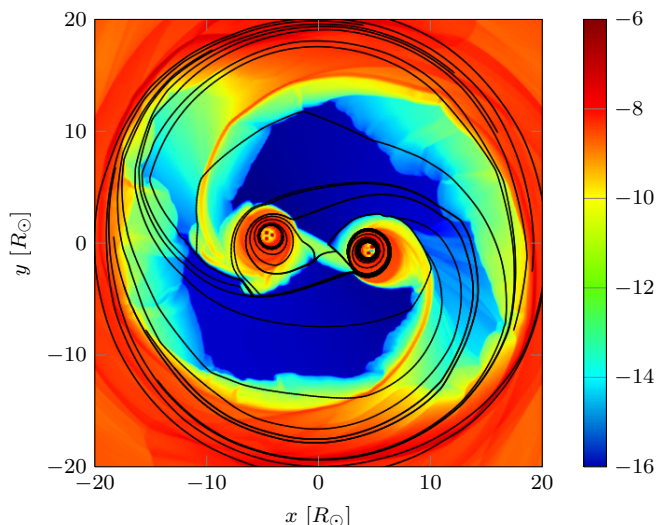


Figure 6. Surface density map in logarithmic scale with flow lines for the V4046 Sgr simulation shown in Fig. 3.

In the case of no mass transfer to the secondary, this component will spiral inwards and eventually be swallowed by the primary. It has sometimes been speculated that mass accretion in systems with low mass secondaries would occur preferentially to the secondary, and that this process could prevent a rapid merging of the components. Our calculations show that the overall process of accretion is the same as in systems of mass ratio close to one. However, the gas flows to the secondary will slow down the process of merging. In the case of a planetary mass companion one expects perturbations to modify the orbital parameters of the planet that can lead to large-amplitude eccentricity oscillations even for distant planets (Holman & Wiegert 1999).

We conclude that binaries on circular orbits open gaps on short time scales, and that substantial mass accretion takes place also in such systems. The accretion is non-axisymmetric, and gas flows from the surrounding disc

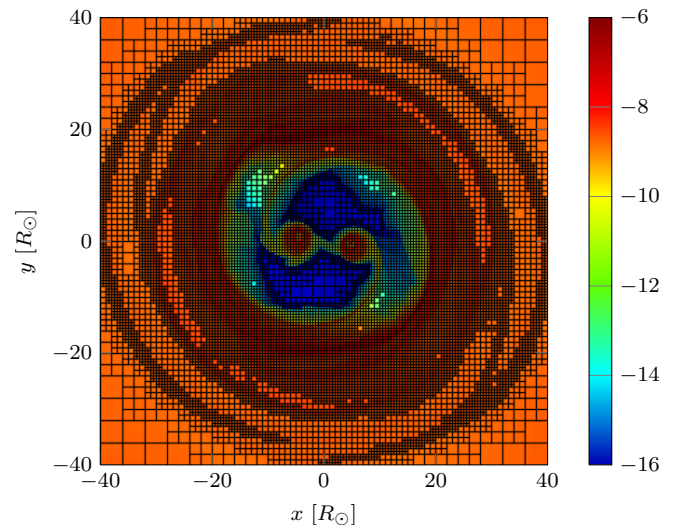


Figure 7. Grid structure with four additional levels of refinement over the density map in logarithmic scale for the same snapshot as shown in Fig. 3. The mesh is refined over the inner cavity and the spiral arms in the circumbinary disc. The colour scale is the same as shown in Fig. 5.

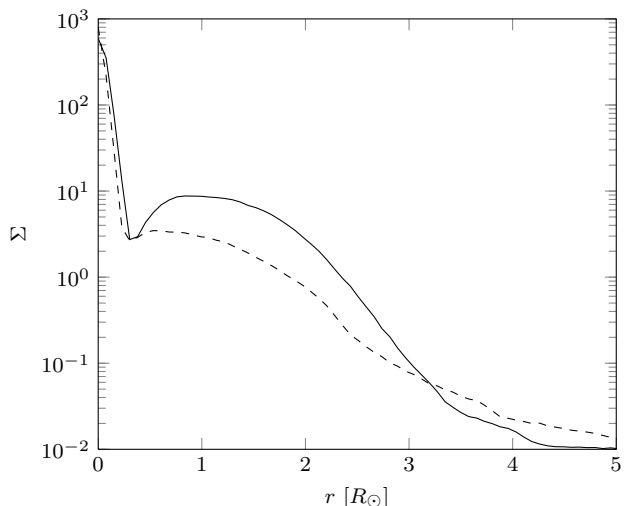


Figure 8. Averaged surface density in logarithmic scale as a function of radial distance in solar radii after 5 orbits. The solid line corresponds to the averaged density around the primary and the dashed line is the density around the secondary. There is a high density peak around each component since we do not consider accretion onto the stars.

through the co-linear Lagrangian points, similar to what was found by Stempels & Gahm (2004) from high-velocity components in the Balmer emission lines of the object. The accretion rate is larger towards the primary, and its accretion disc is more massive than the disc around the secondary in agreement with the simulations by Ochi et al. (2005).

3.2 Eccentric Binaries

In this section we present the results of high-resolution simulations of a binary with components of nearly equal mass

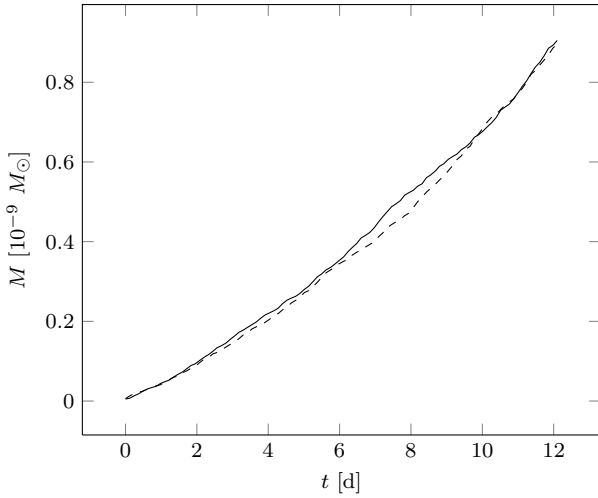


Figure 9. Mass accreted around the primary (solid line) and secondary (dashed line) components as a function of time for the circular binary system V4046 Sgr.

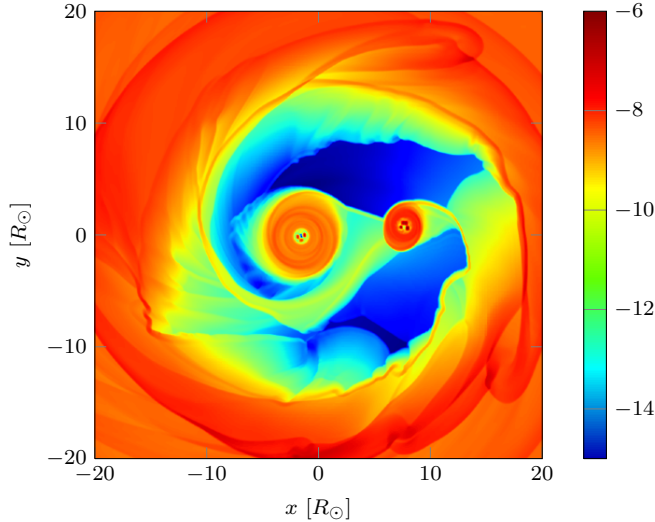


Figure 10. Surface density map in logarithmic scale for a simulation of a circular binary system with a mass ratio of 1:5 and with the same notations as in Fig. 3.

on a highly eccentric orbit. We have selected the parameters for DQ Tau as a case study with the orbital parameters given in Table 2. As in the case of circular orbits we used a grid structure with a dynamically refined grid with four additional levels of refinement. The inner cavity is refined and has higher resolution than the outer regions in the circumbinary disc. The surface density in logarithmic scale is shown in Fig. 11 at periastron and apastron. The location of the cavity rim in the system after it has reached a quasi-static configuration is consistent with the prediction by Artymowicz & Lubow (1996). The shape of the gap depends on the eccentricity of the system and the disc viscosity (Artymowicz et al. 1991). The spiral arms in the outer circumbinary disc become more pronounced than in the V4046 Sgr high-resolution simulations despite the presence of a wave damping region close to the outer boundary, which are not seen

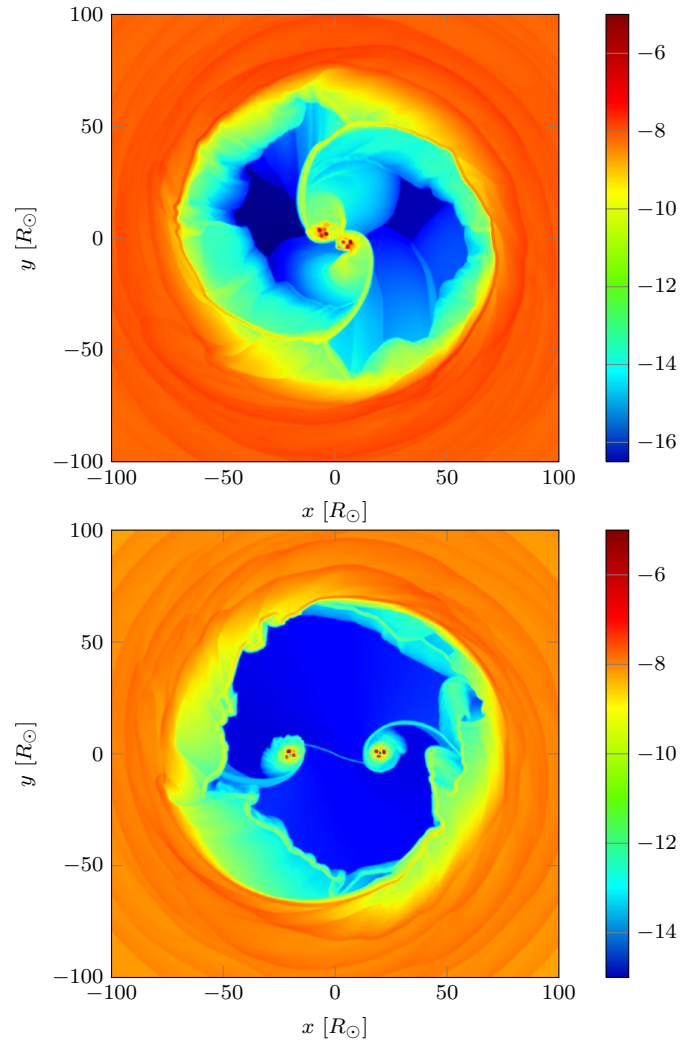


Figure 11. Surface density maps in logarithmic scale for the eccentric binary system DQ Tau in periastron (top) and apastron position (bottom).

in the circular binary simulations with a mass ratio close to unity.

The size of the Roche lobe expands and contracts as the separation between the components changes. Hence, the circumbinary discs are small compared with the circular binary simulations since the closest approach between the stars is only $5.8 R_{\odot}$. There is substantial mass transfer between the discs as the secondary approaches periastron and the spiral arms are truncated as shown in the early calculations by Artymowicz & Lubow (1996). Such periodic changes in the accretion rates onto the stars have also been observed and may produce phase modulations in the line emission (Rozyczka & Laughlin 1997).

From our simulations we derive an averaged accretion rate onto the primary of $8.1 \times 10^{-9} M_{\odot} \text{ yr}^{-1}$, and $6.2 \times 10^{-9} M_{\odot} \text{ yr}^{-1}$ for the secondary. Averaged accretion rates onto the primary are higher than on the secondary in agreement with the dual-grid eccentric binary simulations by Günther & Kley (2002). However, the averaged accretion onto the stellar components agree in order of magnitude with respect to circular binary simulations presented in Sec-

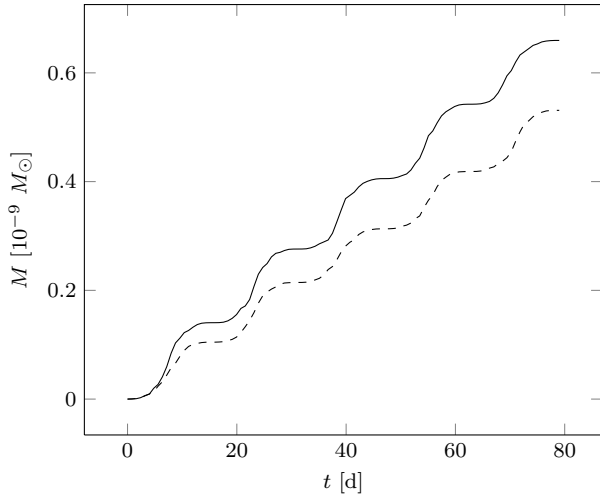


Figure 12. Time dependence of the accreted mass onto the primary (solid line) and secondary (dashed line) components of the DQ Tau system.

tion 3.1. Accreted mass onto the primary and secondary components for the DQ Tau model is shown in Fig. 12. The accretion rates are larger during periastron passage which can explain periodic changes in the observed luminosity. Averaged accretion rates in the orbital plane also agree within order of magnitude with the values obtained from observed luminosities of DQ Tau by Gullbring et al. (1998).

Orbital parameters of the binary system may be changed by stream flows that modify the angular momentum of the orbit (Artymowicz et al. 1991). Although we evolve the binary orbit using an N-body solver that includes the effects of the disc gravity, we are not able to study the orbit evolution for sufficiently long time scales in our model. Considering the orbital evolution of the system would require a simplified hydrodynamic description of the circumbinary disc which is outside the scope of this study.

The patterns of gas flows around circular and eccentric binaries are similar, but with some notable differences as seen when comparing the density distributions shown in Fig. 3 and Fig. 11. In the eccentric case shock fronts in the streams from the disc edge to the stars produce narrow peaks in the density map, and these can be traced as they spiral around each stellar component before matter settle down in the local discs. These discs are smaller than in the circular case since the close approach at periastron prevents the formation of massive circumstellar discs. In the eccentric case the central region is also connected with the disc by bars of low density and perpendicular to the flow direction. Only in the circular case with a mass ratio close to unity a stable central bar connects the circumstellar discs. Spiral patterns develop in both the circular and eccentric cases, but are more pronounced in the latter. In highly eccentric systems such as DQ Tau, spiral arms are formed around each stellar component, although the spiral patterns are torn off as the system nears periastron.

4 COMPARISONS WITH OBSERVATIONS

High-resolution observations of V4046 Sgr and DQ Tau show that the overall appearance of emission line spectra in close TTS binaries are similar to those of single TTS. Both V4046 Sgr and DQ Tau show emission features that are clearly connected to the stellar components, and which vary in projected radial velocity as the stars move around the centre of mass. This emission is certainly local, and the result of enhanced chromospheric activity and accretion induced emission at the footprints of the accretion funnels. However, these stars differ from single stars in that they show periodic fluctuations in extended line wings of the Balmer emission lines coming from warm gas flowing in the circumbinary gap. This emission is a manifestation of tidal dissipation and viscous heating in the accretion flow in the gap, and is powered also from other energetic events in the regions and from photoionization from UV light from the stars. The infrared excess emission comes from the cool, dusty circumbinary disc, while there is no evidence of warm dust in the gap from the energy distributions of the stars in question.

In the case of V4046 Sgr, Stempels & Gahm (2004) found that the Balmer lines have two broad emission components ($\Delta v \sim 170 \text{ km s}^{-1}$) related to gas moving in corotation close to the co-linear Lagrangian points of the system and with projected velocity amplitudes of $\sim 80 \text{ km s}^{-1}$. These components are optically thin, especially in the higher Balmer lines, since the Balmer decrement, as measured for the higher Balmer lines, is more or less constant as a function of velocity shift over the line wings. The computations also indicate a much lower gas density in the accretion flow than for accreting single stars, and since the flow has gained a large spread in projected velocity, photons can easily escape from any site.

However, in our computations we did not consider details of heating or cooling of the gas. As a consequence the gas flows are cool over the entire region, with temperatures below 1000 K, and no H emission can arise. In order to make a first qualitative comparison between calculated and observed line profiles for V4046 Sgr we apply a different equation-of state for the region inside the disc edge, where the H emission is formed. Fig. 13 shows the density and velocity structure of such a modified model assuming a constant $T = 6000 \text{ K}$ in the gap. Compared to the previous models the distributions of surface density and velocity remain the same (see Fig. 3).

In order to estimate expected emission line fluxes from the model we assume that the disc has a fixed geometrical thickness. The scale height of the disc may change from the disc edge to the interior, but these variations can be expected to be moderate and do not affect the final qualitative comparison. Furthermore, the gas density is low and the projected velocity range is large. To characterize the line emission as a function of orbital phase, we use the obtained circumstellar density distribution and assume that the optically thin emission proceeds from the accretion flows in the inner cavity. Since the line emission can be assumed to be optically thin, in the higher Balmer lines, except for the inner cores, we can assume that the line emissivity per volume is proportional to the volume emission measure ($V n_e^2$). Hence, the total line flux within a certain velocity interval is proportional to the surface density squared, Σ^2 , integrated

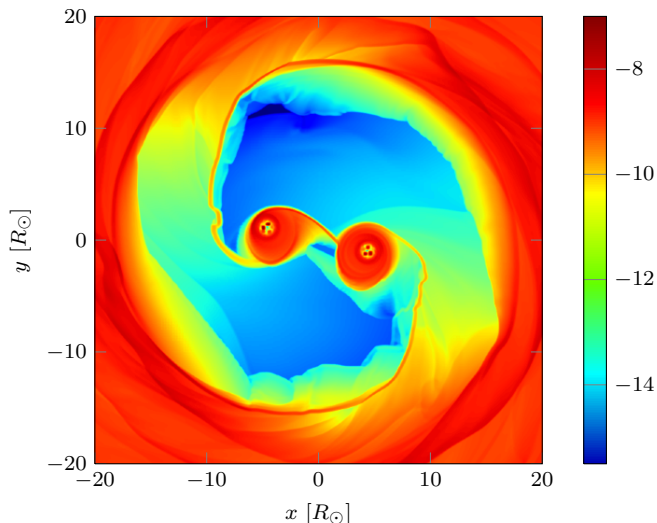


Figure 13. Surface density map in logarithmic scale for a simulation of the system V4046 Sgr after 5 orbits assuming a constant $T = 6000$ K in the gap.

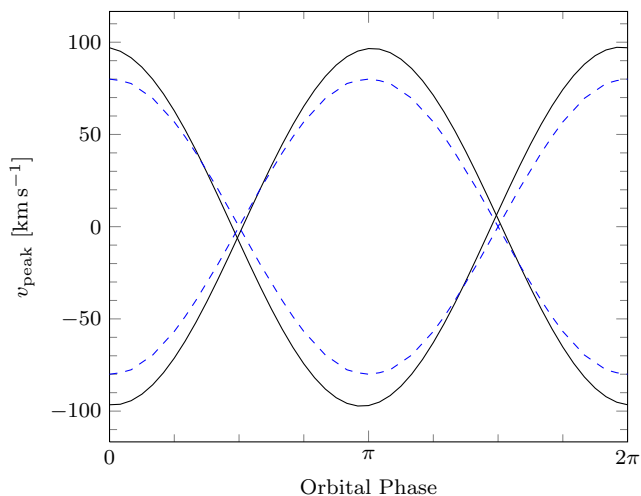


Figure 14. Peak velocities of the line profiles as a function of orbital phase for the V4046 Sgr simulation. The solid lines show the $v\Sigma^2$ weighted averages from the streams onto the primary and secondary components. The peak velocities of the high velocity Gaussian components from the observations are shown by the dashed blue lines. Here, phase zero is defined as the time when the secondary passes the plane of the sky in the direction towards the observer.

over the area confined by the velocity interval in question. No specific statements about the thickness of the accreting layer are needed, since the total line intensities are scaled to match the model profiles.

Our models predict that gas is moving through the co-linear Lagrangian points of the system, just as inferred from the periodic changes observed in the wings of the Balmer lines. We have computed theoretical emission line profiles sampled over different areas inside the gap as a function of phase, and as viewed in the line-of-sight to V4046 Sgr. The best agreement between observed and modelled line profiles, and their variations, appears when in the model the emis-

sion is sampled only from the area inside the disk edge, at an outer radius close to the 2:1 resonance at $1.6a$, and extending inwards over the Lagrangian points in question, to an inner radius of $0.8a$. However, the exact locations of these radii are not very critical for obtaining a fair agreement between observed and modelled peak velocity and line widths. Fig. 14 compares the peak velocities as a function of phase as derived from the model synthetic profiles with those observed by Stempels & Gahm (2004), as described by their empirical multi-component solution to the optically thin H_8 , H_9 and H_{10} Balmer lines, and excluding the stellar components. The model amplitude is 20% larger than the peak velocity of the high velocity wings from the Gaussian decomposition of the observed profiles. However, the relative phases of the peak velocities in the calculation agree well with the observational data.

When also the central discs are included in the computations, strong peaks in the line profiles at velocities extending to 200 km s^{-1} are created. These high velocity components are present at all phases, but are not visible at all in the observed profiles. Hence, only by removing the contributions from the stellar discs and their immediate surroundings, we obtain synthetic line profiles that resemble the observed ones for different phases.

We conclude that there is no observational evidence of any local discs, but that a fair qualitative agreement between observed and modelled properties can be obtained when these discs are removed. Then the remarkable observed changes in the line profiles can be understood in terms of perturbations in a circumbinary disc from which non-axisymmetric gas flows are generated. The accreted material crosses the gap through the saddle points of the potential down to a certain radius outside the orbiting discs. The peaks of the observed line profiles at phases close to 0.0 and 0.5 in Fig. 14 differ from the model in the sense that the model profiles are located at somewhat larger absolute velocities than observed.

If the local discs are geometrically very thin their contribution to the line emission might be very small and the corresponding high velocity components might escape detection. As noted by Basri et al. (1997), most of the spectral properties of TTS do not depend on whether the objects are single or not. Narrow line components and continuous emission (veiling) can be present in both cases and are usually related to magnetospheric accretion. We speculate that the absence of local discs around the stars is related to magnetospheric accretion that could dominate the accretion closer to the stars. Here, matter is channeled along magnetic dipole fields to the polar regions of each star, and the magnetic configuration co-rotates with the stars at relatively low speed.

Carlqvist and Gahm (unpublished) calculated the combined magnetic field configurations resulting from two magnetic binary components. An example is found in Fig. 23 in Petrov et al. (2001) for a binary with a large mass ratio. However, calculations were made also for systems similar to V4046 Sgr and DQ Tau, and with different assumptions on the ratio of the magnetic moments. These calculations show that each star maintains a pronounced local magnetosphere over an area in the disk plane comparable to the size of the local disks present in our numerical simulations. Further out from the stars the global magnetic field strength declines roughly as r^{-3} , and is comparatively very weak at the cir-

cumbinary disk edge. More detailed numerical simulations of the combined magnetic fields in orbiting close TTS binaries, and their interaction with surrounding plasma, have not been done so far.

Another aspect is that closer to the stellar surfaces the gas is further heated and Balmer emission is not any more the dominant emission component. The presence of hot central zones, in for example V4046 Sgr, is confirmed by observations of variable FUV emission lines of He II, C IV and Si IV (de La Reza et al. 1986) as well as significant X-ray emission (Günther et al. 2006).

In the case of DQ Tau our model indicates that there is substantial accretion through the inner cavity onto the stars in agreement with previous SPH simulations (Artymowicz & Lubow 1996). Accretion onto the stars increases significantly as they approach periastron in our simulations of close eccentric systems. This can explain the periodic outbursts in the emission lines and the continuous emission (veiling) observed by Basri et al. (1997), and the sudden brightening at millimetre wavelengths observed by Salter et al. (2008). Basri et al. (1997) also discovered that H_α shows enhanced red wings at phases near periastron. Since no detailed line profile decomposition has been done so far, it is unclear how these variations in line shape can be related to our model. In addition, they found that mass ejection from the system could occasionally occur in periastron. We note that Huerta et al. (2005) found that the forbidden line emission does not change with phase, indicating that this emission originates outside the immediate vicinity of the stars. Carr et al. (2001) found evidence that also cool molecular gas is moving inside the disc gap.

5 CONCLUSIONS

We have presented high-resolution simulations of mass accretion from a circumbinary disc onto a close binary system. We selected orbital parameters from two T Tauri binaries, namely the circular spectroscopic system V4046 Sgr and the highly eccentric system DQ Tau, in order to compare model predictions with observed quantities. These systems have components of nearly equal mass. In addition we study a circular system with a low mass companion. The systems were evolved for long time scales using an adaptive grid method and quasi-stationary solutions were achieved in all cases after a few orbits. We have considered the dynamics and evolution of the discs and gas flows inside the circumbinary gap. The circumbinary disc edge is located close to the 2:1 resonance in agreement with the results from Artymowicz & Lubow (1994).

These calculations confirm that significant gas accretion occur through tidal gaps generated in such systems, in particular in the case of circular orbits but with considerably lower surface densities compared to the systems having highly eccentric orbits. The gas flows are non-axisymmetric in the studied systems, with two gas streams passing the co-linear Lagrangian points on the way down to the stars, where circumstellar discs develop. However, the size of the gap stays constant due to the equilibrium between viscous and resonant torques. In the V4046 Sgr case, spiral arms appear in the circumstellar disc due to the strong gravita-

tional torques from the close stellar component, with a high density bar joining the circumstellar discs.

We find that the local circumstellar disc around the primary is significantly more massive than the disc of the secondary in our simulations after several orbital periods when the system has reached a quasi-static state. Hence, mass accretion goes preferentially to the primary, in accordance with the conclusions by Ochi et al. (2005). In eccentric systems such as DQ Tau, the circumstellar discs are cut off as the system approaches periastron. Part of the material is then accreted onto the stellar cores and accretion rates increase. These periodic accretion changes and brightening events have been observed in DQ Tau (Basri et al. 1997) and confirmed by numerical simulations (Günther & Kley 2002). During apastron the stars accrete mass from the circumstellar discs that form around each star.

We also used our simulation for a simple, qualitative comparison between line emission from the region within the circumbinary disk and the profiles observed by Stempels & Gahm (2004). We found that a fair agreement with the velocity changes as a function of orbital phase observed for the optically thin higher Balmer lines can be achieved if an inner region surrounding the local circumstellar discs, is not taken into account. Our model can characterize the stream flows in the inner cavity of circumbinary discs down to a certain radius from the centre. This shows that in T Tauri binary systems accretion may occur due to gravitational interaction with the circumbinary disc. Since there is no observational evidence for the presence of circumstellar discs, we speculate that hydrodynamic accretion can be effective only down to a certain radius from the centre, below which magnetospheric accretion is likely to take over the accretion process. Our calculations of combined magnetic field configurations around binary magnetic stars also show that each component is surrounded by rather compact local magnetospheres, but that the field strengths decline rapidly towards the circumbinary disk edge.

There are also a number of differences in observed and modelled line profiles and the projected velocities at peak intensity, but only at certain phases. The comparison shows that gas emission is produced in a larger region in co-rotation with the stars than predicted by the model. Three-dimensional hydrodynamic models with self-consistent radiative transfer will be necessary to better estimate line emission from this object and provide constraints on the parameters of the system by matching observed profiles. Future calculations should also include a more realistic mechanism to account for accretion onto the stars.

ACKNOWLEDGEMENTS

MdVB was supported by a SAO predoctoral fellowship and a NOT/IAC scholarship during the course of this project. The code used in this work is developed in part by the U.S. Department of Energy under Grant No. B523820 to the Center for Astrophysical Thermonuclear Flashes at the University of Chicago. This work has made use of NASA's ADS Bibliographic Services. We thank Per Carlqvist for contributing with calculations of combined magnetospheres, and Garrelt Mellema for comments and suggestions. We are grateful to

the anonymous referee for helpful comments that improved the manuscript.

REFERENCES

- Artymowicz, P. 2005, private communication
- Artymowicz, P., Clarke, C. J., Lubow, S. H., & Pringle, J. E. 1991, *ApJ*, 370, L35
- Artymowicz, P. & Lubow, S. H. 1994, *ApJ*, 421, 651
- Artymowicz, P. & Lubow, S. H. 1996, *ApJ*, 467, L77
- Basri, G., Johns-Krull, C. M., & Mathieu, R. D. 1997, *AJ*, 114, 781
- Bate, M. R. & Bonnell, I. A. 1997, *MNRAS*, 285, 33
- Carr, J. S., Mathieu, R. D., & Najita, J. R. 2001, *ApJ*, 551, 454
- Clarke, C. J. 2008, in *Astronomical Society of the Pacific Conference Series*, Vol. 390, *Pathways Through an Eclectic Universe*, ed. J. H. Knapen, T. J. Mahoney, & A. Vazdekis, 76
- de La Reza, R., Quast, G., Torres, C. A. O., et al. 1986, in *ESA Special Publication*, Vol. 263, *New Insights in Astrophysics. Eight Years of UV Astronomy with IUE*, ed. E. J. Rolfe, 107
- de Val-Borro, M., Artymowicz, P., D’Angelo, G., & Pepliński, A. 2007, *A&A*, 471, 1043
- de Val-Borro, M., Edgar, R. G., Artymowicz, P., et al. 2006, *MNRAS*, 370, 529
- de Val-Borro, M., Karovska, M., & Sasselov, D. 2009, *ApJ*, 700, 1148
- Delgado-Donate, E. J., Clarke, C. J., Bate, M. R., & Hodgkin, S. T. 2004, *MNRAS*, 351, 617
- Duchêne, G., Delgado-Donate, E., Haisch, Jr., K. E., Loinard, L., & Rodríguez, L. F. 2007, in *Protostars and Planets V*, ed. B. Reipurth, D. Jewitt, & K. Keil, 379
- Fryxell, B., Olson, K., Ricker, P., et al. 2000, *ApJS*, 131, 273
- Gahm, G. 2006, *Ap&SS*, 304, 149
- Goodwin, S. P., Kroupa, P., Goodman, A., & Burkert, A. 2007, in *Protostars and Planets V*, ed. B. Reipurth, D. Jewitt, & K. Keil, 133
- Gullbring, E., Hartmann, L., Briceno, C., & Calvet, N. 1998, *ApJ*, 492, 323
- Günther, H. M., Liefke, C., Schmitt, J. H. M. M., Robrade, J., & Ness, J.-U. 2006, *A&A*, 459, L29
- Günther, R. & Kley, W. 2002, *A&A*, 387, 550
- Günther, R., Schäfer, C., & Kley, W. 2004, *A&A*, 423, 559
- Hanawa, T., Ochi, Y., & Ando, K. 2010, *ApJ*, 708, 485
- Hayasaki, K., Mineshige, S., & Sudou, H. 2007, *PASJ*, 59, 427
- Holman, M. J. & Wiegert, P. A. 1999, *AJ*, 117, 621
- Huerta, M., Hartigan, P., & White, R. J. 2005, *AJ*, 129, 985
- Kastner, J. H., Zuckerman, B., Hily-Blant, P., & Forveille, T. 2008, *A&A*, 492, 469
- Kley, W. 1998, *A&A*, 338, L37
- Kley, W., D’Angelo, G., & Henning, T. 2001, *ApJ*, 547, 457
- Lin, D. N. C. & Papaloizou, J. 1985, in *Protostars and Planets II*, ed. D. C. Black & M. S. Matthews, 981
- Martín, E. L., Magazzù, A., Delfosse, X., & Mathieu, R. D. 2005, *A&A*, 429, 939
- Mathieu, R. D., Ghez, A. M., Jensen, E. L. N., & Simon, M. 2000, *Protostars and Planets IV*, 703
- Mathieu, R. D., Stassun, K., Basri, G., et al. 1997, *AJ*, 113, 1841
- Ochi, Y., Sugimoto, K., & Hanawa, T. 2005, *ApJ*, 623, 922
- Papaloizou, J. C. B. & Terquem, C. 1995, *MNRAS*, 274, 987
- Pepliński, A., Artymowicz, P., & Mellema, G. 2008, *MNRAS*, 386, 164
- Petrov, P. P., Gahm, G. F., Gameiro, J. F., et al. 2001, *A&A*, 369, 993
- Quast, G. R., Torres, C. A. O., de La Reza, R., da Silva, L., & Mayor, M. 2000, in *IAU Symposium*, Vol. 200, *IAU Symposium*, 28
- Reid, I. N. & Gizis, J. E. 1997, *AJ*, 113, 2246
- Rozyczka, M. & Laughlin, G. 1997, in *Astronomical Society of the Pacific Conference Series*, Vol. 121, *IAU Colloq. 163: Accretion Phenomena and Related Outflows*, ed. D. T. Wickramasinghe, G. V. Bicknell, & L. Ferrario, 792
- Salter, D. M., Hogerheijde, M. R., & Blake, G. A. 2008, *A&A*, 492, L21
- Sotnikova, N. Y. & Grinin, V. P. 2007, *Astronomy Letters*, 33, 594
- Stempels, H. C. & Gahm, G. F. 2004, *A&A*, 421, 1159